

Subproject B2.11

Correlation Effects and Disorder in Nanostructure Devices

Principal Investigators: Alexander Mirlin

CFN-Financed Scientists: Dmitry Aristov, Dmitry Gutman, Stephane Ngo Dinh, Sam Carr

Further Scientists: Dmitry Bagrets, Ferdinand Evers, Igor Gornyi, Achim Mildenberger, Boris Narozhny, Pavel Ostrovsky, Dmitry Polyakov, Thomas Ludwig, Martin Schneider

**Institut für Theorie der Kondensierten Materie
Karlsruhe Institute for Technology, Campus South**

**Institut für Nanotechnologie
Karlsruhe Institute for Technology, Campus North**

Correlation Effects and Disorder in Nanostructure Devices

Introduction and Summary

This project is centered around effects of strong Coulomb interactions and disorder in nanoscopic systems. Electron interactions effects become especially important when the system size and dimensionality is reduced. This is also true for interference phenomena in disordered systems. Thus, correlations and disorder phenomena play a prominent role in nanostructures, strongly affecting their electronic properties.

Originally, the activity was focussed on transport and magnetic properties of **strongly interacting quantum dot systems**, with a particular emphasis on the **Kondo effect** in various setups. Using analytical and numerical techniques, in particular, the renormalization group approach, we have investigated the Kondo physics and **quantum phase transitions** in nano-devices [B2.11:9].

More recently, the focus of research carried out within the project has largely shifted towards **one-dimensional and quasi-one-dimensional nanostructures**. Strongly correlated electron systems in one dimension (1D) [1] have become an area of immense interest from the perspective of both fundamental and technological aspects of nanophysics. In recent years, progress in nanofabrication technologies has made it possible to manufacture a variety of single- and few-channel quantum wires connected to the electric leads and to perform systematic transport measurements on the very narrow wires. The experimental realizations of quantum wires include, in particular, carbon nanotubes [2-13], semiconductor [14,15] and metallic [16,17] nanowires, and polymer nanofibers [18,19]. Central to the fascinating physics of such 1D systems is that electron-electron interactions can have dramatic effects leading to the emergence of a strongly correlated state --- **Luttinger liquid (LL)**. The latter constitutes a canonical example of a non-Fermi liquid, in which quasiparticle fermionic excitations are inappropriate to describe low-energy physics. At the foundation of the conventional Luttinger liquid theory is the description in terms of elementary excitations (plasmons, spinons). While the bosonization approach [1] had facilitated significant progress in studying Luttinger liquids, a number of most fundamental properties of these systems remained largely unexplored. These include **quantum interference, localization, and decoherence phenomena**, effects induced by **curvature of electron dispersion**, as well as **non-equilibrium physics**. These properties of quantum wires have been investigated within the present project. We have also studied transport and magnetic properties of so-called "**ladder**" structures which are a generalization of strictly 1D chains and are relevant to a class of organic quasi-1D materials.

Another direction of our recent and current activity is related to transport in **two-dimensional (2D) nanostructures**. Particularly important is the research on transport properties of a monoatomic graphite layer -- **graphene**. Recent breakthrough in fabrication of this material and consequent transport measurements have triggered an outbreak of research activity in the field of graphene physics, both on experimental and theoretical side. In a very short time a new area of research has emerged and become one of key research directions in the material science and condensed matter physics. A hallmark of graphene is its unconventional electronic spectrum: the low-energy excitations are 2D "relativistic" **Dirac fermions**. This leads to remarkable electronic properties of this material revealed by transport measurements. In particular, graphene shows anomalous, half-integer quantum Hall effect, which is related to the Berry phase of relativistic carriers. Also, it was found that the quantum Hall effect in graphene can be observed up to room temperature, whereas it disappears at 30 K in the best semiconductor structures. Another remarkable discovery is that the

conductivity of the undoped graphene in a broad temperature range (from 300 K down to 30 mK) is essentially independent of T and has a value close to the quantum e^2/h (times four, which is the total spin/valley degeneracy). From the point of view of applications, it is important that the electron concentration in graphene can be varied by a gate, making possible to realize a field-effect transistor. Further, a gap can be engineered and tuned in graphene-based structures. Moreover, it is possible to realize a room-temperature single-electron transistor on the basis of graphene. These findings open a way for development of novel **graphene-based nanoelectronics**. Further discussed applications include spin and Josephson qubits, composite materials, and sensors for individual molecules. In view of the outstanding importance of this direction, the graphene-related activity was split in the year 2007 into a separate project (B2.14, later B1.8). Our research in the field of 2D structures included also the investigation of **disorder-induced quantum phase transitions** (Anderson localization) and corresponding critical phenomena, as well as the study of quantum effects of **electron-electron interactions** on transport properties of disordered 2D electron systems.

1. Kondo Effect and Impurity Quantum Phase Transition in Nano-Devices

This research direction was led by M. Vojta who was a Principal Investigator until Summer 2006.

Considerable progress was achieved [B2.11:1, B2.11:7, B2.11:8, B2.11:9, B2.11:10] by using analytical and numerical renormalization group (RG) techniques, including a newly developed analytical RG approach. This has allowed us to study systematically the physics of the Kondo effect in nano-devices, in particular, quantum phase transitions and corresponding critical behavior, multichannel Kondo and non-Fermi liquid physics, and Kondo quantum dots coupled to unconventional superconductors. A review on impurity quantum phase transitions can be found in [B2.11:9].

1.1. Quantum phase transitions in the pseudogap Kondo model

Quantum phase transitions in Kondo-type models can be realized if Kondo screening, well known in metallic systems, is suppressed even at zero temperature. In a single-channel situation, a straightforward possibility is to reduce the electron bath density of states at the Fermi level to zero. The absence of low-energy states then prevents screening for small Kondo couplings.

A paradigmatic model is the so-called pseudogap Kondo model, with a power-law bath density of states $\sim|\omega|^r$. Since the 1990s, various mean-field and numerical methods have been applied to this model, which consistently show that for all $r>0$ there is a quantum phase transition as function of the Kondo coupling. However, the critical behavior seemed to depend on the value of r and on the presence or absence of particle-hole symmetry and was not understood beyond numerics, except for small r . In previous work, we have solved this problem: Re-writing the model in the language of the corresponding Anderson Hamiltonian allowed us to develop controlled perturbative expansions, which, if combined with renormalization-group methods, are suitable to deduce the critical behavior for all r . In particular, $r=1$ turned out to play the role of an upper-critical dimension. Excellent agreement with numerics was obtained.

In [B2.11:7], we have combined these RG methods with Callan-Symanzik equations in order to calculate not only critical exponents and universal amplitudes, but full crossover functions, both at and away from criticality. While temperature-dependent static and zero-temperature dynamic quantities can be calculated in a straightforward manner, and agree nicely with numerics, the regime of finite-temperature low-frequency dynamics is notoriously difficult. Nevertheless, we were able to

make progress by a suitable renormalization procedure in the Callan-Symanzik framework. Our analytical understanding of the critical behavior of the pseudogap Kondo model can be used to analyze numerical results, in particular those obtained by Wilson's numerical renormalization group (NRG).

1.2. Non-Fermi-liquids in double quantum dots

The two-impurity Kondo model is known to display a quantum phase transition between Kondo-screened impurity spins and an inter-impurity singlet state. The quantum-critical non-Fermi liquid state, arising at the phase transition point, has strong similarities to the famous two-channel Kondo effect. In [B2.11:10], we have proposed a realization of this non-Fermi liquid state in double quantum-dot systems, Fig.1a. We have found that, contrary to the common belief, the corresponding fixed point is robust against particle-hole and various other asymmetries, and is only unstable to charge transfer between the two dots.

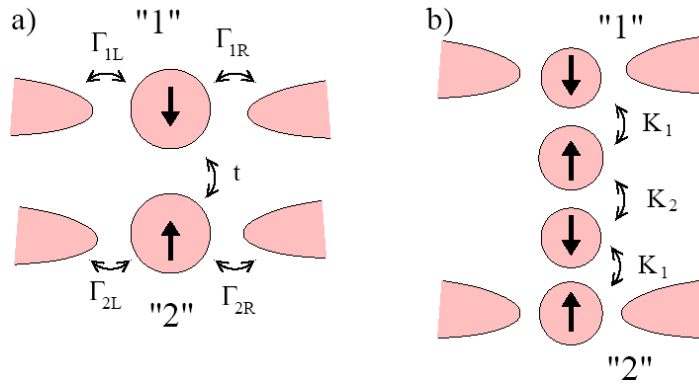


Fig 1. a) System of two quantum dots to realize a non-Fermi liquid state [33]. b) Modified set-up with suppressed charge transfer processes, with an even number of quantum dots inserted between the two main dots (1,2) attached to leads.

In order to efficiently suppress such charge transfer, we have proposed an experimental set-up with additional quantum dots inserted in between the main dots (Fig.1b)– these additional dots acts like an antiferromagnetic Mott insulator which mediates spin coupling, but no charge coupling. Estimates show that this modified set-up allows a controlled approach to the quantum critical state, using present-day semiconductor nano-technology. Finally, we have calculated transport and scaling properties in the vicinity of the critical point [B2.11:10].

1.3. Kondo effect in interacting environments

Exotic forms of the Kondo effect can be realized if an impurity is embedded in an interacting system. An example is the physics of magnetic moments embedded in Mott insulators, with is of some relevance to spintronics applications. In the absence of magnetic order in the host, the question of paramagnetic screening (as in the metallic case) arises. For conventional paramagnets with spinon confinement, earlier work has shown that true screening does not arise, neither in the gapped paramagnetic phase nor at the bulk quantum critical point towards antiferromagnetic order. In [B2.11:1], we have introduced a novel class of Kondo problems where the impurity interacts with deconfined spinons of an exotic spin liquid. Combining RG and large-N methods, we were able to show that true screening is possible here. This provides an interesting avenue to detect spin-liquid phases in frustrated magnets.

2. Correlations and Disorder in 1D and Quasi-1D Nanostructures

2.1. Quantum Interference in Strongly Correlated 1D Quantum Wires (Luttinger Liquids) with Impurities

Mesoscopic physics of strongly correlated electrons is one of the most important and promising directions of current research on 1D electron systems. Recent transport measurements on carbon nanotubes [11] reported both sample-dependent conductance fluctuations and strong magnetoconductivity, in qualitative similarity to the mesoscopic phenomena in higher-dimensional disordered electron systems. In Ref. [11], electron transport through the nanotubes displayed features characteristic of the crossover from ballistic conduction to a disorder-dominated regime. Furthermore, in the past few years techniques to grow nanotubes of size up to the millimeterscale [12,13]---much larger than the typical value of the disorder-induced mean free path---have been developed. First transport measurements [12,13] on the ultralong nanotubes provided evidence for disorder-induced diffusive motion of electrons in a wide range of temperature. Altogether, these advances have paved the way for systematic experimental study of disorder, interference, and localization phenomena in 1D, motivating the theoretical activity within the present project.

An important milestone in realization of the project was a development of the theory of transport of interacting electrons in a quantum wire with impurities (disordered LL) [B2.11:12]. We have shown that the key notion of the mesoscopic physics -- weak localization -- is applicable to a strongly correlated 1D system and calculated the relevant dephasing rate. It was found that for spinless (spin-polarized) electrons the weak localization dephasing rate is governed by the interplay of electron-electron interaction and disorder, thus vanishing in the clean limit. Specifically, the weak-localization correction to the conductivity has the form

$$\sigma^{\text{wl}} = -\frac{1}{4} \sigma^{\text{D}} \left(\frac{\tau_{\phi}^{\text{wl}}}{\tau} \right)^2 \ln \frac{\tau}{\tau_{\phi}^{\text{wl}}} \propto \frac{1}{\alpha^2 T} \ln(\alpha^2 T),$$

where the weak-localization dephasing rate is given by

$$\frac{1}{\tau_{\phi}^{\text{wl}}} = \alpha \left(\frac{\pi T}{\tau} \right)^{1/2}, \quad T \gg T_1 = \frac{1}{\alpha^2 \tau},$$

α is the interaction strength, T is the temperature, and τ the elastic mean free time. We have also demonstrated that the weak localization dephasing rate is parametrically different from the one governing the damping of Aharonov-Bohm oscillations in the ring geometry. Two alternative approaches to the problem were developed, both combining fermionic and bosonic treatment of the underlying physics. The first method is a two-step procedure which combines the bosonic renormalization-group treatment of high-energy renormalization processes at the first step with the subsequent analysis of low-energy real processes in the fermionic language. The other approach is based on the method of "functional bosonization" which makes it possible to treat both types of effects simultaneously. The findings of [B2.11:12] are of conceptual importance, showing that the famous non-Fermi-liquid character of the LL does not prevent this system from exhibiting the features characteristic of conventional mesoscopic electron structures. This work has provided a framework for a systematic study of mesoscopic effects in strongly correlated electron systems.

In Ref. [B2.11:25] we have explored the influence of spin on the quantum interference of interacting electrons in a single-channel disordered quantum wire. The nature of the electron interference in a spinful LL is particularly nontrivial because the elementary bosonic excitations that carry charge and spin propagate with different velocities. We have extended the functional bosonization approach to treat the fermionic and bosonic degrees of freedom in a disordered spinful LL on an equal footing. We have analyzed the effect of spin-charge separation at finite temperature both on the spectral properties of single-particle fermionic excitations and on the conductivity of a disordered quantum wire. It was demonstrated that the notion of weak localization, related to the interference of multiple-scattered electron waves and their decoherence due to electron-electron scattering, remains applicable to the spin-charge separated system. The relevant dephasing length, governed by the interplay of electron-electron inelastic scattering and spin-charge separation, was found to be parametrically shorter than in a spinless Luttinger liquid. We have calculated both the quantum (weak localization) and classical (memory effect) corrections to the conductivity of a disordered spinful LL, which determine the temperature dependence of the conductivity.

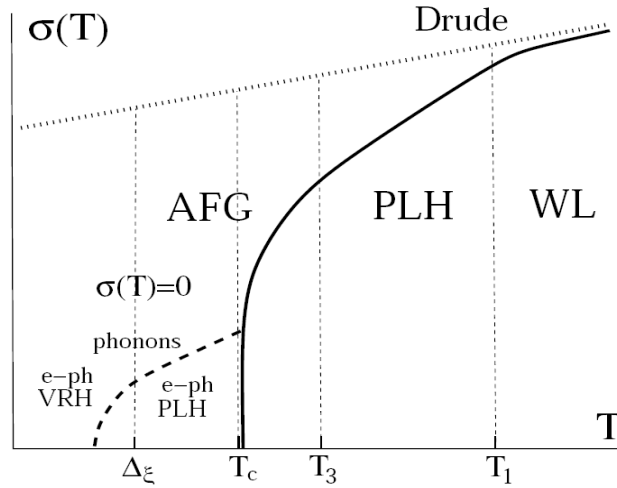


Fig. 2. Schematic view of temperature dependence of conductivity of an interacting disordered 1D system (disordered Luttinger liquid) on the log-log scale. High temperature: WL -- weak localization regime; intermediate temperature: PLH -- power-law hopping, low temperature: AFG -- Anderson-Fock glass. In the presence of weak electron-phonon coupling, the low-temperature conductivity is of variable-range hopping form with a small prefactor governed by phonons (e-ph VRH).

In Ref. [B2.11:16] we have studied the situation of a very strong repulsive electron-electron interaction. We have shown that in this case there are two distinct disorder-induced mechanisms that limit the mobility of the system with lowering temperature: classical pinning and quantum localization. We have determined characteristic length and temperature scales at which each of these competing mechanisms becomes operative.

2.2. Spectral Nonlinearity in Quantum Wires and Coulomb Drag

In theoretical investigations of quantum wires, the usual simplification is the linearization of the fermionic dispersion near the Fermi level. This allows one to fully take into account the electronic interaction in wires and leads eventually to a notion of Luttinger liquid (LL). The curvature of the

fermionic dispersion is considered as the irrelevant perturbation which is not important at low temperatures, and is discarded in most theoretical studies. However, several physical effects --- most notably, Coulomb drag [25] --- are observable due to combined presence of the curvature and interaction. Thus, it is necessary to develop a theory capable of incorporating both these features.

The usual (fermionic) approach is to take the curvature into account exactly and to treat the interaction as a perturbation. Proceeding this way, one is unable to consider the domain of low temperatures where the interaction effects are most important. Within this subproject, we have developed an alternative approach [B2.11:15] which is based on the bosonization technique and fully takes interaction into account, treating curvature as a perturbation. The bosonization technique usually starts with linearization of fermionic dispersion and describes electrons as complicated combinations of densities (plasmons). When the curvature of fermionic dispersion is included, it induces a decay of plasmon modes, which can be considered in perturbation theory [26].

In the work [B2.11:15], modifications in density correlation functions due to curvature were investigated at finite temperature T . We have also established correspondences between the bosonization and the fermionic approaches in those regimes where both methods are applicable.

In particular, we have shown that perturbative treatment of curvature within the bosonization approach always reveals singularities at the "light cone" of linearized dispersion, which is an intrinsic feature connected with the non-Lorentzian shape of density correlation functions. We have demonstrated that these singularities are unimportant for the calculation of observables at lowest T but become a dominant feature at higher T , where the usual fermionic approach is more appropriate. We have argued that in the consistent bosonization approach to the curvature one should separate different plasmon decay terms in two kinds. The first kind is present even in a non-interacting system and becomes increasingly more important at high T . The second kind appears only if both interaction and curvature are present, and dominates the physics at lowest T .

The most important application of our approach was the analysis of the Coulomb drag by small momentum transfer between two clean LL, which is only possible due to curvature. This analysis has extended previous results on the drag resistivity, obtained in [27] within the framework of usual fermionic approach. Specifically, we have found the T -dependence of drag resistivity, $R_{12} \sim T^2$ at high temperatures and $R_{12} \sim T^5$ at low temperatures, and determined the corresponding prefactors. Our results show the efficiency of bosonization at low T , when the electron correlations are particularly important.

2.3. Ladder Structures

The so-called ladder systems are perhaps the simplest generalization of strictly one-dimensional chains. They consist of two chains ("legs") which are connected by "rungs" providing hopping of electrons between the legs as well as their interaction. Experimental realizations of ladder systems were first discovered in copper oxides, and then in various organic materials. One should expect nano-fabricated samples with ladder geometry in foreseeable future. All this has motivated the interest of theoreticians' interest to ladder systems. The main focus of theoretical investigation of the last decade was connected with the *symmetrical* ladders, where two or more legs were identical. At the same time, organic materials of PNNNO family [28] show a structure of a "necklace" of blocks attached to the main chain, see Fig. 3. We have studied this class of structures within the present subproject and have shown that they reveal a rich phase diagram.

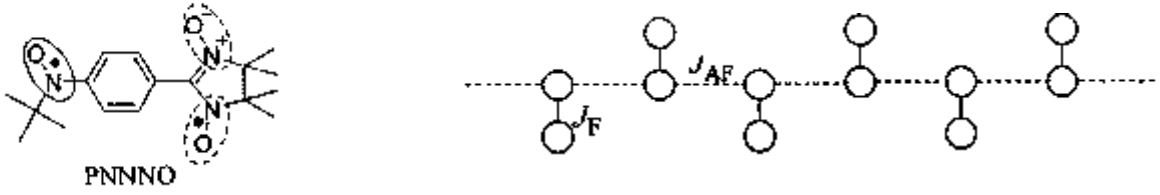


Fig. 3. Molecular structure of the organic biradical crystals PNNNO is shown on the left. The description in terms of the effective model ("centipede ladder") is shown on the right.

Despite, the overall 1D geometry, an analytical investigation of the single-pole ladder is not a simple task. One faces a typical difficulty of the "necklace" geometry, when the description of the long-range properties of the main chain should take into account extremely localized degrees of freedom of the dangling spins. In the work [B2.11:18, B2] we have analyzed a spin-1/2 ladder with a ferromagnetic rung coupling and inequivalent antiferromagnetically (AF) coupled chains. By decreasing the AF exchange along one of the legs, we have investigated a smooth crossover between the conventional symmetric ladder and the extreme case of "centipede" ladder presented in Fig. 3. We have shown that during this crossover the ground state has a finite string order parameter characterizing the Haldane phase. Close to the "centipede" situation we find a new energy scale, which we interpret in terms of a Suhl-Nakamura interaction of localized spins *via* the magnon continuum of the main chain. As a consequence, we observe a crossover in the scaling of the spin gap at weak coupling from $\Delta \sim J_F$ for symmetric ladder to $\Delta \sim J_F^2/J_{AF}$ for single-pole situation. Those results are obtained on the basis of large scale Quantum Monte Carlo calculations. In particular, we have studied the evolution of the non-local string order parameter and have shown that its behavior is largely decoupled from one of the energy gap in the spectrum. A more complete analysis of the problem was carried out in the subsequent publication [B2.11:31] on the basis of numerical results obtained by exact diagonalization, density matrix renormalization group and Quantum Monte Carlo simulations. It was found that strongly asymmetric ladders are characterized at small J_F by two energy scales: the exponentially small spin gap $\sim J_F \exp(-J_{AF}/J_F)$ and the bandwidth of the low-lying excitations induced by a Suhl-Nakamura indirect exchange $\sim J_F^2/J_{AF}$.

The above magnetic ladder is formally obtained for a half-filled electronic system with strong on-site Hubbard repulsion. To get insight into the peculiarities of kinetic degrees of freedom in the "centipede" geometry, we have also investigated such ladder at one quarter electronic filling per site [B2.11:13]. Specifically, we have demonstrated that the ferromagnetic rung coupling leads to instability towards dimerization and with the possibility of subsequent coherent propagation of charge transfer excitons. Unlike the cases known from the literature, where a dimerization mechanism is either explicitly built-in within the Heisenberg chain Hamiltonian or else, arises as a result of competition between the nearest and next nearest exchange coupling, in our case the dimerization occurs as a result of competition between the on-rung hopping and exchange coupling.

2.4 Interaction and impurities in fermionic ladders

Another direction of research activity related to correlated ladder structures was pursued in Ref. [40]. We studied the effect of a local external potential on a system of two parallel spin-polarized nanowires placed close to each other (two-leg ladder). We analyzed first the nature of the ground state of the system in the absence of impurities. The evolution of the corresponding phase diagram

(in the plane of intra-chain and inter-chain interaction parameters) with increasing inter-chain hopping is shown in Fig. 4.

We analyze now the effect of a local perturbation. Remarkably, we find that in the physical case of repulsive interaction transport properties of the system are highly sensitive to the transverse gradient of the perturbation: the asymmetric component grows under renormalization and at $T = 0$ completely suppresses conductance in contrast with the symmetric potential that remains transparent (Fig. 5). While any realistic potential will have some asymmetry, if this is sufficiently small there will be a wide temperature window in which it remains weak. We envisage a possible application of the unusual property discovered in our work in the sensitive measurement of local potential field gradients.

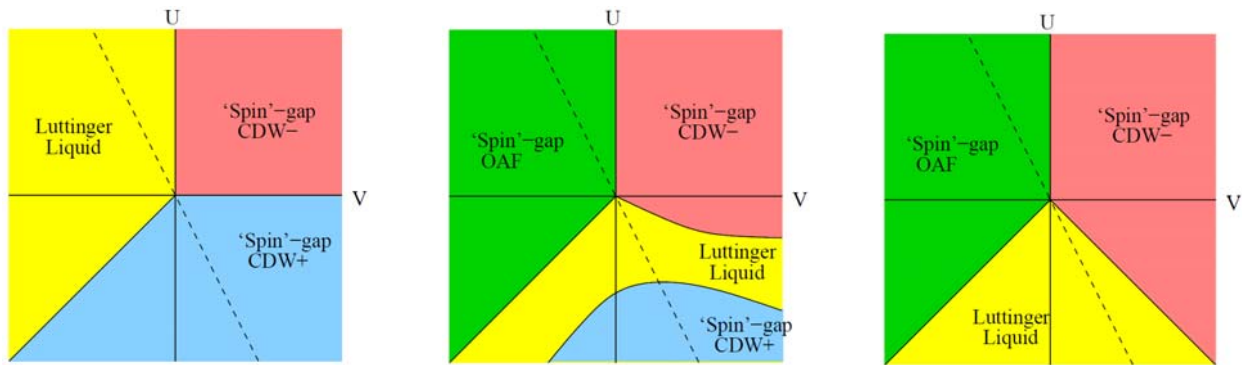


Fig. 4. Phase diagrams of two-leg fermionic ladders (in the absence of impurities). From left to right: zero, small, and large inter-chain hopping. V and U are the intra- and inter-chain nearest-neighbor interaction constants.

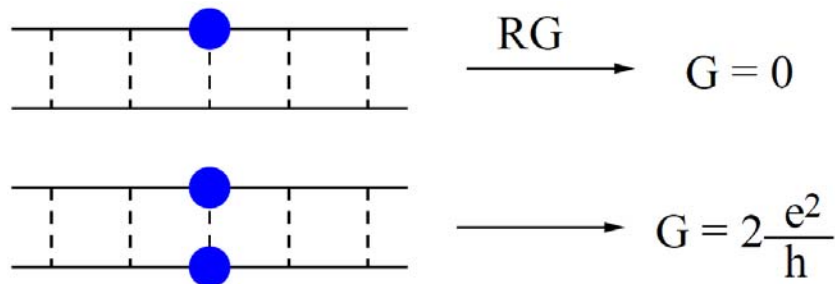


Fig. 5. Two-leg repulsive ladder ($U, V > 0$) with local perturbation. Remarkably, for a single impurity (*top*) interaction drives the conductance to zero under renormalization, while for symmetric impurities (*bottom*) the conductance remains at its maximum value.

2.5 Aharonov-Bohm conductance through a tunnel-coupled Luttinger liquid ring

In Ref. [B2.11:31] we studied the effect of electron-electron interaction on transport through a tunnel-coupled single-channel ring. Direct confrontation of a theory of transport through a LL Aharonov-Bohm ring with experiment appears now to be possible since many-electron nanorings with a few or single conducting channels have been manufactured [37,38].

We have demonstrated that e-e interactions lead to profound and unusual effects in transport through a single-channel quantum-ring interferometer tunnel-coupled to the leads, originating from the phenomenon of persistent-current blockade. We have shown that the conductance as a function of magnetic flux exhibits a series of sharp resonances broadened by dephasing, the distance between which is controlled by the interaction strength (Fig. 6). The physics behind this behavior is the blocking of the tunneling current by the circular current. We have calculated the main contribution to the dephasing rate, which is due to tunneling-induced fluctuations of the circular current. The physics described in the paper remains intact for spinful electrons and ballistic systems with a small number of conducting channels. Our predictions can thus be verified by measuring the conductance of a semiconductor nanoring or a single coil of carbon nanotube.

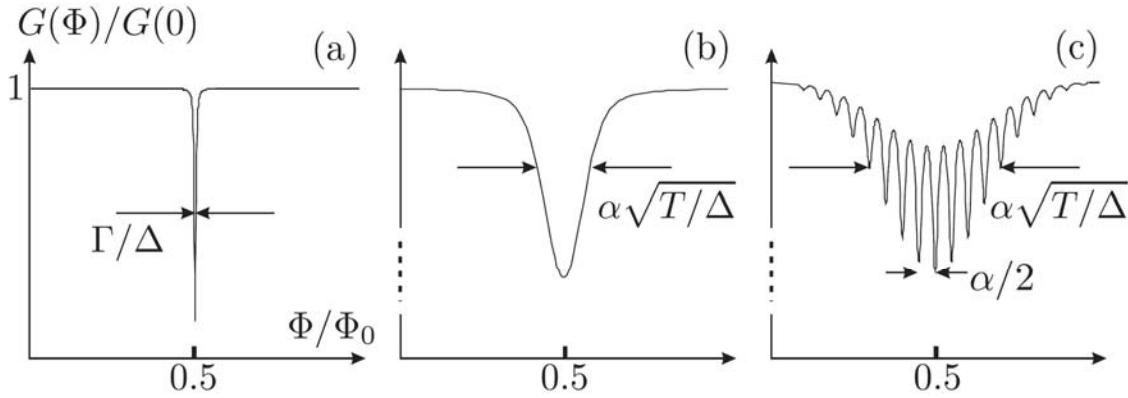


Fig. 6. Conductance G of a LL Aharonov-Bohm ring as function of magnetic flux shows series of anti-resonances that survive thermal averaging. Evolution of the flux-dependence of the conductance with increasing interaction strength is shown.

2.6 Tunneling into Luttinger liquid: Beyond the leading order in tunnel coupling.

In Ref. [B2.11:34] we studied how electron-electron interactions renormalize tunneling into a Luttinger liquid beyond the lowest order in the tunneling amplitude (Fig.7). We have demonstrated that the commonly accepted picture of tunneling into a LL is qualitatively modified when the tunneling amplitude is not treated as infinitesimally small. We considered the case of weak interaction that allowed us to use the fermionic renormalization group method for all values of conductances. We have found that the conventional fixed point has a finite basin of attraction only in the point contact model, but a finite size of the contact makes it generically unstable to the tunneling-induced break up of the liquid into two independent parts (Fig.8, left). In the course of renormalization to the nonperturbative-in-tunneling fixed point, the tunneling conductance may show a nonmonotonic behavior with temperature or bias voltage (Fig.8, right). Our predictions can be verified by systematically varying the distance to the tunnel electrode in experiments on carbon nanotubes or semiconductor nanowires.

In order to address the Y junction in the case of arbitrary interaction strength, one will have to use the bosonization methods. A step forward in this direction was done in [39]; the further work is currently in progress.

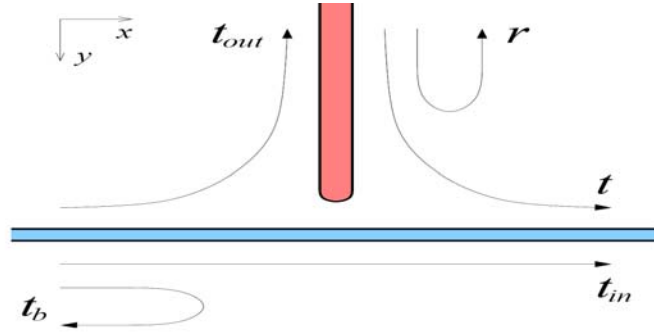


Fig. 7. Junction between a quantum wire (horizontal) and a tunnel electrode (vertical). The arrows denote the scattering processes (and their amplitudes) for incoming electrons.

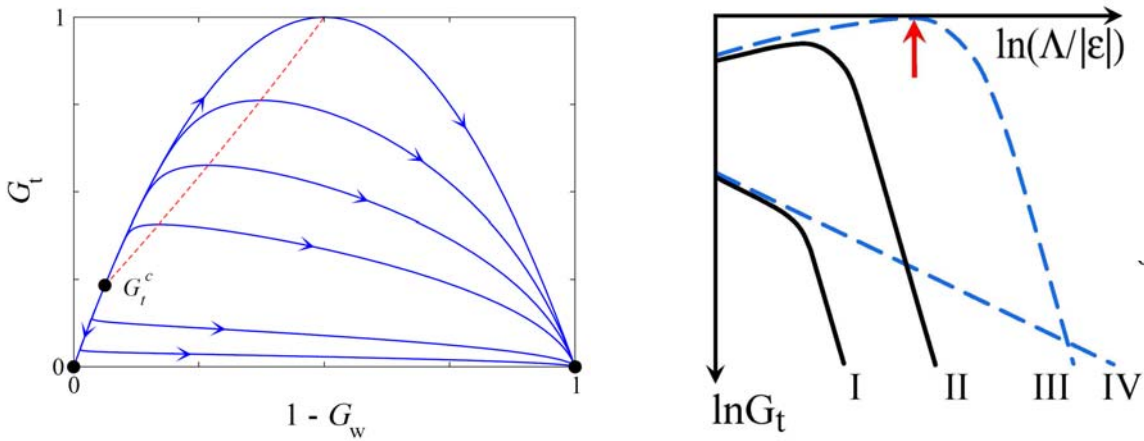


Fig.8. *Left:* Renormalization group flow for the LL tunnel junction: G_t is the tunnel conductance and G_w the wire conductance. Only stable fixed point ($G_t=0, G_w=0$): break up of the tunnel junction into 3 independent parts with enhanced ZBA (right). *Right:* Tunnel conductance G_t and wire conductance G_w may show nonmonotonic behavior as a function of bias voltage or temperature (middle and right).

3. Non-Equilibrium Physics in Quantum Wires

One of the goals of the project was to address the *non-equilibrium* phenomena in low-dimensional conductors with strong electron-electron correlations, in particular, in one-dimensional (1D) quantum wires, exhibiting the LL behaviour. We started our research in this direction by developing the theory of tunneling into a disordered film out of equilibrium [B2.11:17]. This has allowed us to explore the non-equilibrium zero-bias anomaly (ZBA). In Ref. [B2.11:24, B2.11:27] we have extended this formalism to (clean) 1D wires (LLs). We have analyzed several setups where strongly non-equilibrium Luttinger liquid can be formed and developed the theory of tunneling ZBA for such out-of-equilibrium quantum wires. The full solution of the problem of a non-equilibrium LL with arbitrary energy distributions of incoming electrons was achieved in Refs. [B2.11:28, B2.11:30] where the method of non-equilibrium bosonization was developed. This has allowed us to obtain exact results for tunnelling spectroscopy [B2.11:28, B2.11:30], as well as for counting statistics [B2.11:33] of a LL conductor. In Refs. [B2.11:20, B2.11:26] we have made step forward in development of the kinetic theory of the *disordered* LL out of equilibrium. In the work

[B2.11:29] we have studied tunnelling spectroscopy of a biased quantum wire with a single impurity.

3.1. Zero-bias anomaly in a non-equilibrium disordered conductor

The suppression of tunneling current at low bias due to electron-electron interaction is known as the zero bias anomaly (ZBA). The theory of ZBA for disordered metals at thermal equilibrium has been developed in [29]. Recently, the tunneling spectroscopy technique has been developed that allows one to explore experimentally Keldysh Green functions of an interacting system that carry information about both tunneling density of states and energy distribution.

Recent measurements of the tunneling density of states (TDOS) in biased quasi-one-dimensional wires [32] have called for an extension of the theory to *non-equilibrium* setups. Such a theory was developed in our work [B2.11:17]. We have started from the Keldysh σ -model and derived an action for real and virtual density fluctuations; an approach having much in common with the functional bosonization. We have shown that the two edges are not independent: one edge affects the ZBA near the other one via real interaction-induced scattering processes governing the dephasing of electrons in the non-equilibrium regime.

Besides the experimental motivation, the problem of ZBA in a non-equilibrium system is of fundamental theoretical interest. At equilibrium, the distribution of electrons in energy has a single edge at the Fermi energy. The Coulomb interaction between the tunnelling electron and the electrons in the Fermi sea excites virtual particle-hole pairs around the Fermi edge, leading to the suppression of the TDOS, similarly to the Debye-Waller factor. The suppression gets stronger when the electron energy approaches the Fermi energy. Out of equilibrium, the distribution of particles may have two (or several) sharp edges, which poses important questions related to interplay of real (inelastic scattering, dephasing) and virtual (renormalization) processes. This problem is a representative of a class of phenomena that involve renormalization away from thermal equilibrium, such as the Fermi edge singularity [30] and the Kondo effect [31].

3.2. Non-equilibrium bosonization of Luttinger liquids: Tunneling spectroscopy and full counting statistics

Recent experiments on carbon nanotubes and quantum Hall edges have proved the efficiency of this technique in the context of 1D systems [33,34]. The technological and experimental advances motivate the theoretical interest in the tunneling spectroscopy of strongly correlated 1D structures away from equilibrium.

In Ref. [B2.11:24] we started to attack the problem of tunnelling spectroscopy of non-equilibrium LL in quantum wires. A clean LL is a remarkable system: it is completely integrable and as such does not exhibit any relaxation to equilibrium. An arbitrary excited state will never decay to the equilibrium state characterized by temperature T in view of absence of any inelastic e-e scattering: the allowed energy transfer is exactly zero [35]. (This is in stark contrast to electron liquids in higher dimensionalities, where the characteristic energy transfer is T .)

Model setups for tunneling spectroscopy of a non-equilibrium LL [B2.11:24] are shown in Fig. 9. We assumed that the interaction strength vanishes towards the ends of the wire. Left- and right-movers are characterized by distribution functions formed in electrodes or with a help of scatterers located at the end of the wire. In the "partially non-equilibrium" setup each of the fermionic distributions is of equilibrium form but with different temperature and chemical potential. In the

"fully non-equilibrium case" each of the fermionic distribution is by itself of a non-equilibrium form. A particularly interesting is the "most nonequilibrium" situation, when these distribution functions may have a double-step form with two sharp Fermi edges. It is remarkable that (in view of the absence of energy relaxation discussed above) such a state of the electron system can be created and preserved despite the strongly correlated character of the LL.

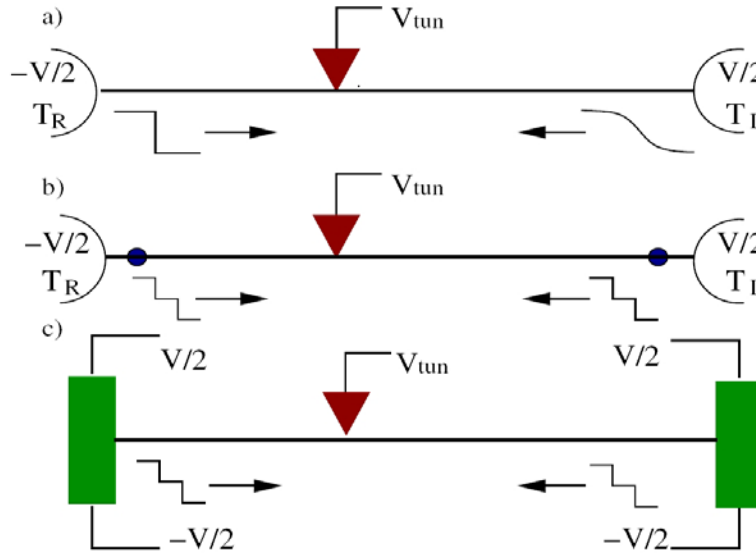


Fig. 9. Setups for studying tunneling into a non-equilibrium Luttinger liquid. The interacting part of the wire is assumed to be clean. (a) "Partially non-equilibrium" LL. Two electrodes are at different temperatures and chemical potentials. (b,c): "Fully non-equilibrium" setups. In (b) the double-step distribution function is formed due to scattering at barriers at the end of the wire, while in (c) the non-equilibrium is formed in reservoirs.

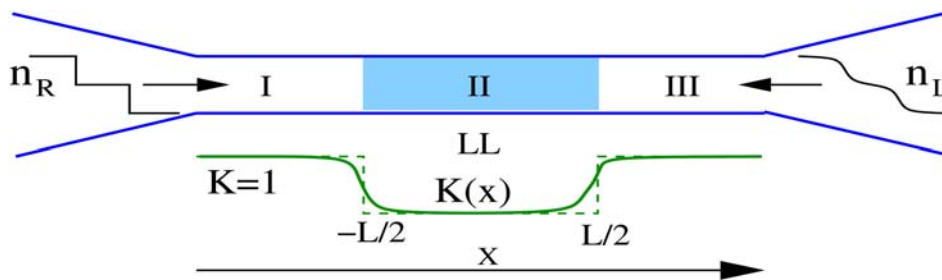


Fig.10. Interacting quantum wire (region II) coupled to two reservoirs with different distribution functions modelled by non-interacting wires (region I and III). The profile of the LL interaction constant $K(x)$ is also shown.

To develop the theory of tunnelling spectroscopy of a non-interacting LL, we model the reservoirs as non-interacting regions I and III (Fig.10). In Ref. [B2.11:27] we have explored the case of partial non-equilibrium (Fig.9a). For this purpose we have used the framework of functional bosonization within which the system is characterized by fermionic and bosonic (plasmons) degrees of freedom. We have calculated Keldysh Green functions G^{\geq} that carry information about the TDOS and the fermionic distribution functions in different parts of the wire. The interaction affects the tunneling

characteristics in three distinct ways, see Fig.11. First, it induces a power-law ZBA in the TDOS (with two dips split by the voltage) in the interacting part of the wire. Second, it leads to broadening of ZBA singularities due to dephasing, with the non-equilibrium dephasing rate governed by the interaction strength and the plasmon distribution inside the wire. The third effect of the interaction is the inelastic scattering of electrons, leading to their redistribution over energies. This effect takes place in those regions where the interaction strength varies in space (i.e. near the wire boundaries), inducing backscattering of plasmons (but not of electrons). This leads to relaxation of the electron distribution functions: left and right moving fermions “partly exchange” their distribution. For slowly varying interaction, when the plasmons with relevant frequencies go through essentially without reflection, the energy relaxation of electrons is negligible. In the opposite limit, when the plasmons are almost entirely reflected (due to strong and sharply switched interaction or, else, due to disordered boundary regions inducing the plasmon localization), the left- and right-movers essentially exchange their distribution functions (but not their total density).

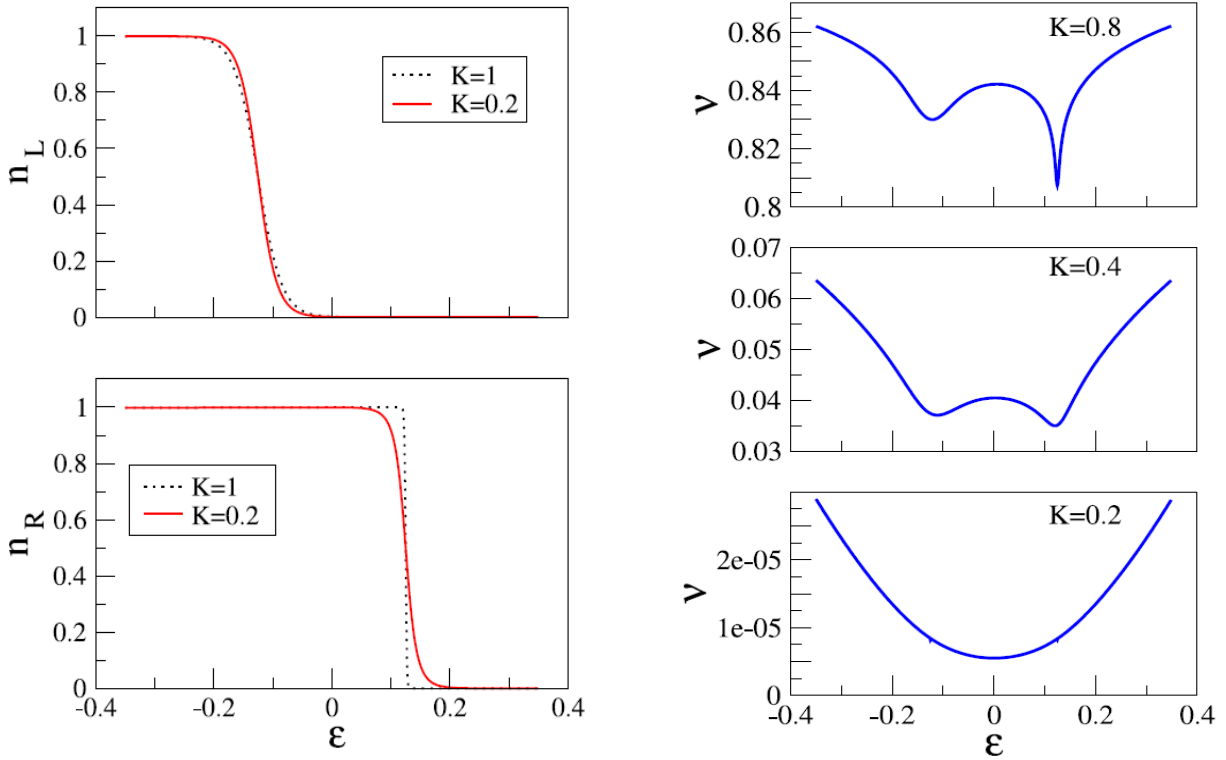


Fig. 11. Tunneling spectroscopy of a LL in partial non-equilibrium. Temperatures of the leads are $T_L = 0.2$ and $T_R = 0.001$; the bias voltage is $eV = 0.25$; sharp boundaries assumed. Shown are electron distribution function (left panel) and TDOS (right panel) in the interacting part of the system (region II). With increasing interaction strength the split ZBA becomes smeared by dephasing.

In Refs. [B2.11:28, B2.11:30] we have achieved an exact solution for the tunnelling spectroscopy of LL with arbitrary distributions of left and right movers. We have developed a novel framework of nonequilibrium bosonization and derived a bosonic theory describing the LL of interacting 1D electrons out of equilibrium. The theory is characterized by an action depending on density fields defined on the Keldysh time contour. In contrast to the equilibrium case, this theory is not Gaussian, which is a manifestation of the fact that the density matrix is nondiagonal in the bosonic Fock

space. We have used this theory to calculate the electronic Green functions which can be measured via tunneling spectroscopy technique and carry the information about energy distribution, zero-bias anomaly, and dephasing, are expressed in terms of functional determinants of single-particle “counting” operators. The corresponding time-dependent scattering phase is found to be intrinsically related to “fractionalization” of electron-hole excitations in the tunneling process and at boundaries with leads (Fig.12, left panel). Results are generalized to the case of spinful particles as well to Green’s functions at different spatial points relevant to the problem of dephasing in LL interferometers. For double-step (or, more generally, multiple-step [36]) distributions, the dephasing rates are oscillatory functions of the interaction strength, see Fig. 12 (right panel). Further, in this situation the power-law exponents are modified by non-equilibrium conditions [36].

In Ref. [B2.11:33] the non-equilibrium bosonization approach was used to study the full counting statistics (FCS) of a LL conductor. The result has a form of counting statistics of non-interacting particles with fractional charges, induced by scattering off the boundaries between the LL wire and the non-interacting leads.

The framework of non-equilibrium bosonization developed in these works should be useful for the theoretical study of a variety of problems related to 1D correlated systems out of equilibrium.

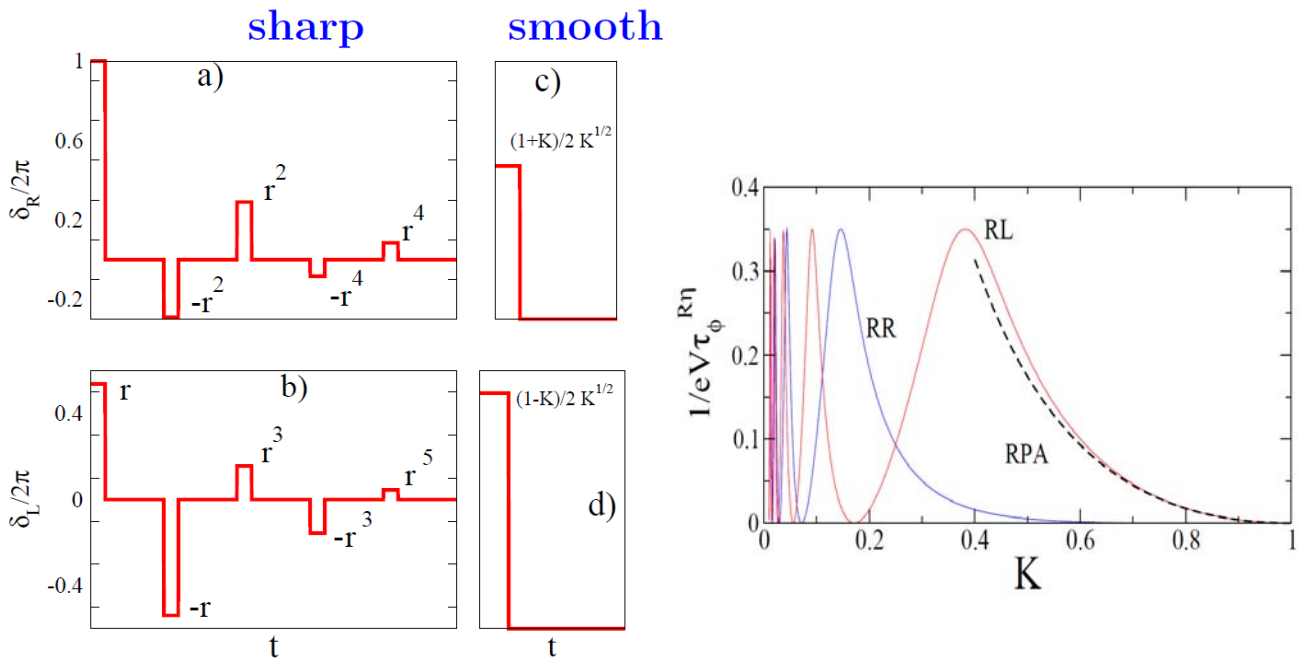


Fig. 12. *Left panel:* fractionalization 2π pulse at the tunneling and at boundaries governs dephasing and energy redistribution in tunneling spectroscopy as well as charge fractionalization in FCS. The time-dependent phases for the tunneling spectroscopy problem are shown, for the cases of smooth and sharp boundaries. *Right panel:* Dephasing rates for double-step distribution are oscillatory functions of the interaction strength (K is the LL interaction parameter).

3.3. Kinetic theory and energy relaxation in a disordered Luttinger liquid

In Refs. [B2.11:20, B2.11:26] we have developed a kinetic theory in the framework of the Luttinger liquid model. As discussed above, there is no equilibration in a homogeneous LL: inelastic

relaxation processes are not allowed. Thus, relaxation to equilibrium due to pairwise e-e collisions in a LL is only possible if momentum conservation is broken by inhomogeneities. Of central importance is therefore the question of how the equilibration in a LL occurs in the presence of a random backscattering potential, which was the subject of our works [5] and [6]. We have developed a *kinetic* approach to nonequilibrium phenomena in a disordered LL, by formulating kinetic equations for *distribution functions*. As has been already emphasized, the crux of the problem is that the conventional scheme of bosonization is not applicable to a generic nonequilibrium state of a LL, and one has to introduce the distribution functions of not only bosonic but also fermionic excitations. Our main result is a set of kinetic equations which describe (i) inelastic e-e scattering, mediated by virtual plasmons, and (ii) creation/annihilation of real plasmons; both processes being only triggered by elastic scattering off disorder. We have calculated the energy-resolved rates of these processes (i.e. collision kernels of the kinetic equations). The kernel $K(\omega)$ of fermion scattering cross-section is shown in Fig. 13 (left panel). As a first application of the kinetic theory, we have calculated a key quantity in nonequilibrium problems: the energy relaxation rate $1/\tau_E$. In a remarkable departure from higher-dimensional Fermi liquids, $1/\tau_E$ in a LL at not too low temperature turns out to be given by the *elastic* scattering rate $1/\tau$. Equilibration in a biased disordered wire is illustrated in Fig. 13 (right panel).

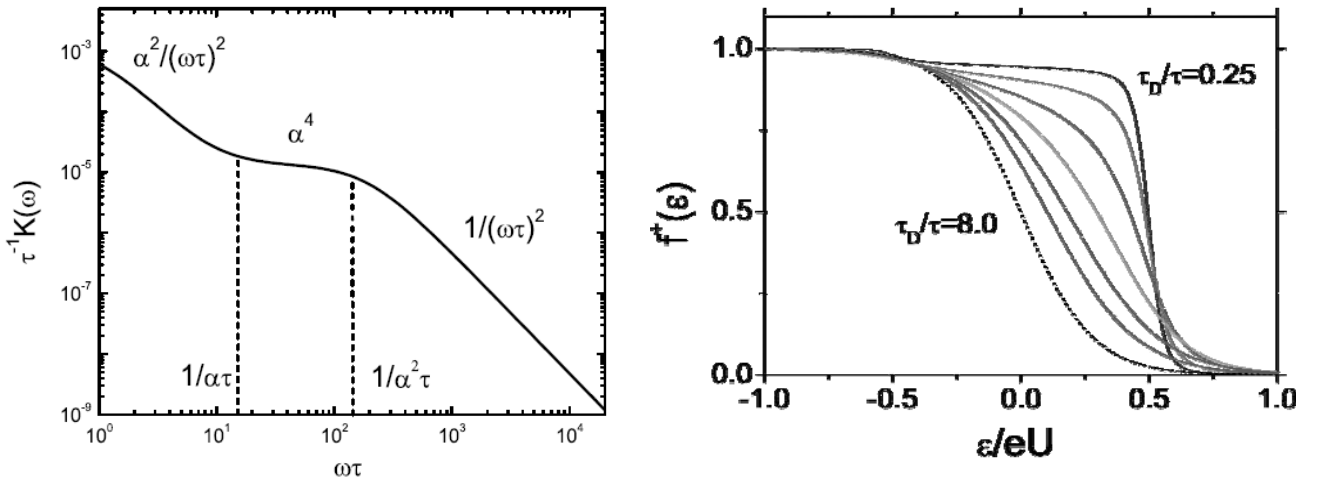


Fig. 13. *Left panel:* Frequency dependence of the total collision kernel, describing the two-fermion scattering in the disordered Luttinger liquid. In the limit $\omega \gg 1/\alpha^2\tau$ the kernel does not contain the interaction strength α , which leads to the energy relaxation rate $1/\tau_E \sim 1/\tau$. *Right panel:* Distribution function of right-moving electrons in the middle of a quantum wire of length L , biased by $eU=40$ T. Solid lines correspond to $\tau_D/\tau = 0.25, 0.5, 1, 2, 4, \text{ and } 8$, where $\tau_D = L/v_F$ and $1/\tau$ is the disorder-induced elastic scattering rate. The dashed curve shows the limiting Fermi distribution. The figure demonstrates that the energy equilibration occurs on the time scale of τ .

3.4 Tunneling spectroscopy of a biased quantum wire with a single impurity

In Ref. [B2.11:29] we evaluated tunneling rates into/from a voltage biased quantum wire containing weak backscattering defect (Fig.14). The problem bears similarity with those discussed in Sec. 3.2; the crucial difference is that in the present case the impurity inducing backscattering which leads to a truly non-equilibrium state of a LL is located within the interacting (LL) region. The backscattering off such an impurity under voltage bias leads the emission of nonequilibrium

plasmons with typical frequency $\omega \leq U$. Contrary to the problems considered in Sec.3.2, where the non-equilibrium distribution was created outside of the interacting part of the system, we were not able to find an exact solution of this problem. We used the functional bosonization formalism in the non-equilibrium (Keldysh) formulation and have developed a real-time instanton approach. Specifically, we have found the field configuration optimizing the action in the absence of impurity and then evaluated the impurity action on this configuration. This approximation is fully controllable for a weak impurity and arbitrary interaction strength. We have found that, similarly to Sec.3.2, the tunneling rates are split into two edges (Fig.15).. While the tunneling exponent at the main edge is equal (in the leading order) to that of equilibrium LL, the exponent at the second edge (shifted by U) is negative for not too strong interaction ($K > 1/3$). This nonequilibrium effect is associated with inelastic electron tunneling accompanied by absorption/emission of real plasmons with a typical frequency $\omega \sim U$. The ZBA singularities are broadened by the non-equilibrium dephasing rate

$$\tau_\phi^{-1} = (2/\pi) U r_U^2 \sin^2 \pi \delta$$

where $\delta = (1 - K)/2$. As for the double-step distributions in the setup of Sec.3.2, the dephasing rate shows oscillatory dependence on the LL interaction constant K ; the specific form is, however, different, which reflects a different type of the non-equilibrium LL state.

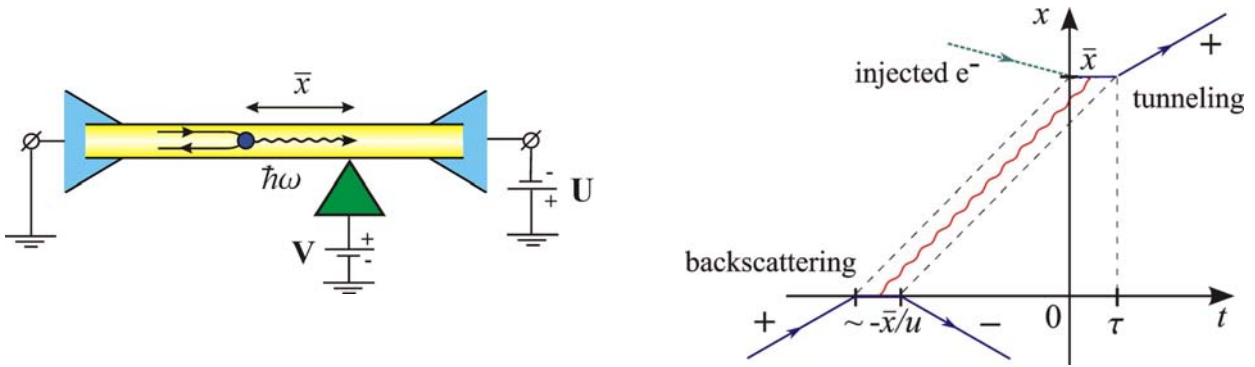


Fig.14. *Left panel:* Tunneling experiment with a voltage biased quantum wire and an impurity. *Right moving electrons* have a larger chemical potential relative to left moving electrons, $\mu_R - \mu_L = U > 0$. *Right panel:* Real plasmons (wavy line) created in the course of inelastic electron backscattering at $t \sim -x/u$, are absorbed by the injected electron at $t \sim 0$.

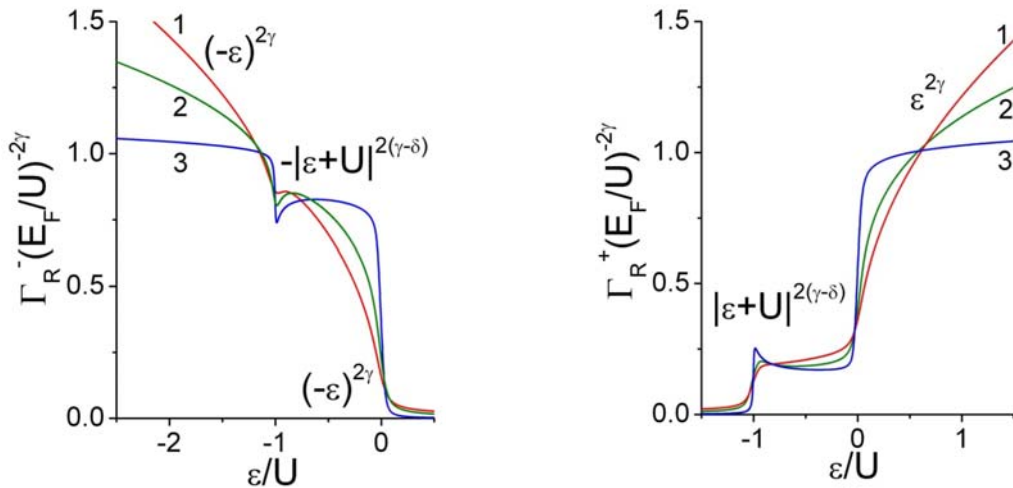


Fig.15. Electron tunneling rates from (*left*) and into (*right*) the non-equilibrium LL, for different interaction strengths: $K = 0.4$ (1), 0.5 (2), 0.75 (3). The ZBA exponents at Fermi edges are shown; $\gamma = (1-K)^2/4K$ is the conventional equilibrium exponent and $\delta = (1 - K)/2$.

The approach developed in this work will be useful for analysis of tunneling and interference in a broad class of nonequilibrium LL structures with impurities and/or tunneling couplings.

4. Two-Dimensional Nanostructures

4.1. Electronic Properties of Graphene Structures with Impurities

We have studied [B2.11:6] electron transport in graphene in the presence of different types of disorder (in particular, charged impurities, dislocations, ripples). We have shown that the nature of disorder is of crucial importance for the behavior of the conductivity. Specifically, it is important (i) whether the individual scatterers are strong or weak and (ii) what is the symmetry of the disorder in the sublattice and valley space. We have used a combination of theoretical approaches, including self-consistent Born approximation, self-consistent T-matrix approximation, and renormalization group. Within the renormalization group approach, we have determined a complete set of one-loop equations governing the evolution of coupling constants for all symmetries of disorder with the length on ballistic scales.

We have shown, that, away from half filling, the concentration dependence of conductivity is linear (with logarithmic corrections) for strong scatterers (unitary limit), $\sigma \sim n_e \ln n_e$, while it is only logarithmic in the case of weak scatterers (Gaussian disorder). We have constructed a "phase diagram", showing which of these types of behavior should be expected for given microscopic parameters of the disorder. For the physically important case of Coulomb impurities and ripples, which are characterized by long-range $1/r$ potentials, the conductivity behavior is linear as for strong impurities (but without logarithmic correction), $\sigma \sim n_e$. The linear behavior of the conductivity obtained for strong and long-rang scatterers agrees with the experimental findings, demonstrating that one of these kinds of disorder is dominant in experimentally studied structures.

At half filling, the conductivity is generically strongly affected by localization effects. However, this is not so for certain special types of disorder symmetry. In particular, in Ref. [B2.11:6] we have analyzed in detail the situation when the randomness preserves one of the chiral symmetries of the clean Hamiltonian. We have shown that for this case ("chiral disorder") the conductivity at the Dirac point is of the order of the conductance quantum and takes a universal value $4e^2/\pi h$. We have also analyzed a frequency dependence of conductivity in this situation. Whether the chiral disorder may indeed dominate in experimentally relevant structures, explaining the observed value of conductivity $\sim e^2/h$ remains an open question. We have found that, alternatively, a value of conductivity $\sim e^2/h$ at the Dirac point can emerge if the dominant disorder does not scatter electrons between the two valleys. Our work in this direction, which has started within the present subproject, was continued within the subproject B2.14 (presently B1.8) devoted to physics of graphene-related nanostructures; a detailed report is presented there.

4.2. Criticality in Disordered 2D Nanostructures

In a series of papers [B2.11:3, B2.11:5, B2.11:14, B2.11:19, B2.11:23], we have studied disorder-induced Anderson localization transitions in 2D structures. The Anderson metal-insulator

transitions represent a famous example of quantum phase transitions and are characterized by very peculiar properties. A particular emphasis in our work was put on phase diagrams for 2D systems of different symmetry classes, critical behavior at localization transitions, and multifractality of critical wave functions. In particular, we have introduced a notion of boundary multifractality for a critical system. Specifically, if one tunnels into a boundary of a structure at the critical point of the Anderson transition, one probes strong fluctuations of the local density of states near the boundary, which are characterized by a distinct set of critical exponents ("boundary multifractality spectrum"). A large body of activity on Anderson transition is summarized in our review [B2.11:22] in the Reviews of Modern Physics.

4.3. Electron-Electron Interaction Effects in 2D Disordered Systems

We have continued the research on effect of electron-electron interactions on transport properties of 2D structures. In [B2.11:2] we have developed a theory of interaction-induced effects in quantum magnetooscillations. We have shown that the electron-electron interaction in a disordered 2D structure induces temperature-dependent quantum corrections to the quantum scattering rate and to the effective mass, that show up in the damping of the magnetooscillations. It was found that the dominant effect is that of the renormalization of the effective electron mass due to the interplay of the interaction and impurity scattering. These results are currently used by many experimental groups for the interpretation of magnetooscillations data (in particular, for extracting the value of the effective mass) and are expected to be useful for understanding the physics of a high-mobility 2D electron gases in the low-density regime (near the apparent metal-insulator transition), where the electron correlation effects are particularly strong.

In Ref. [B2.11:21] we have studied the quantum effects in conductivity of fermions interacting via a Chern-Simons gauge field. This type of electron-electron interaction arises in effective description of certain strongly correlated 2D systems (most notably, half-filled lowest Landau level). We have investigated the interaction-induced transport characteristics --- the quantum correction to conductivity and the dephasing, and analyzed the resulting temperature dependence of the conductivity. In view of the singular character of gauge-field interaction, the renormalization and dephasing effects are particularly strong for these systems. This work has demonstrated the complexity of physics emerging in the field of low-temperature transport and quantum-coherence phenomena in strongly-correlated systems. One can expect that the methods and ideas developed in [B2.11:21] will be useful for the analysis of mesoscopic phenomena in a broad class of low-dimensional strongly-correlated structures.

4.4. Topological phase transitions in 2D structures

We consider a two dimensional model of non-interacting chains of spinless fermions weakly coupled via a small inter-chain hopping and a repulsive inter-chain interaction (Fig. 16, left). The model shows a very rich phase diagram and is a playground for many phases which are sought after by the community of correlated fermions. In particular, the phase diagram of this model has a surprising feature: an abrupt change in the Fermi surface as the interaction is increased. We study in detail this meta-nematic transition, and show that the well-known $2\frac{1}{2}$ -order Lifshitz transition is the critical endpoint of this first order quantum phase transition (Fig.17). Furthermore, in the vicinity of the endpoint, the order parameter has a non-perturbative BCS-like form. We also study a competing crystallization transition in this model (Fig. 16, right), and derive the full phase diagram. This physics can be demonstrated experimentally in dipolar ultra-cold atomic or molecular gases. In the presence of a harmonic trap, it manifests itself as a sharp jump in the density profile.

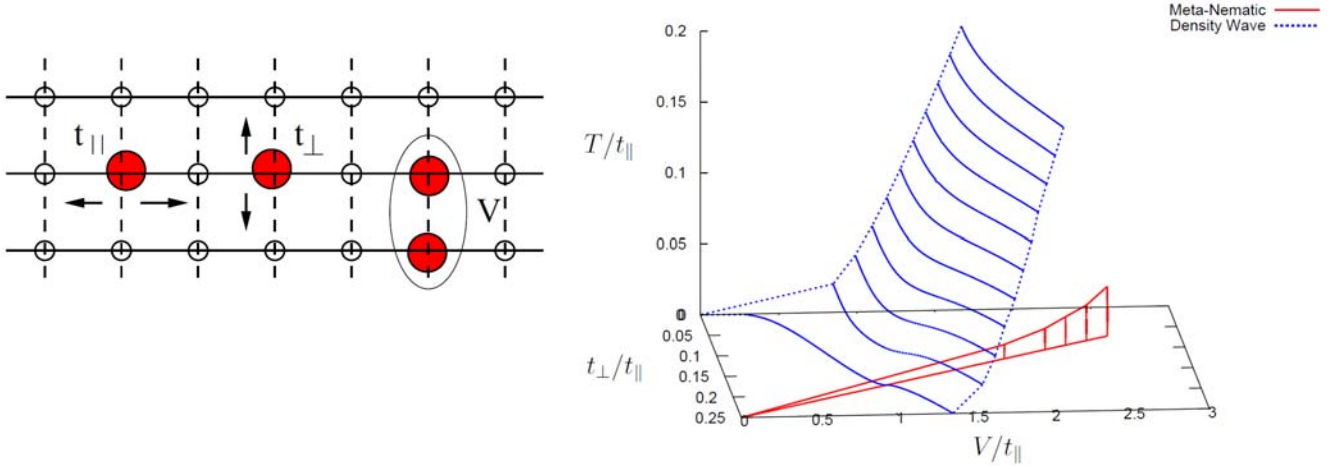


Fig. 16. *Left:* Model: Spinless fermions on a 2D array of chains coupled by inter-chain hopping t_{\perp} and inter-chain interaction V . *Right:* Competing instabilities: meta-nematic and charge-density wave.

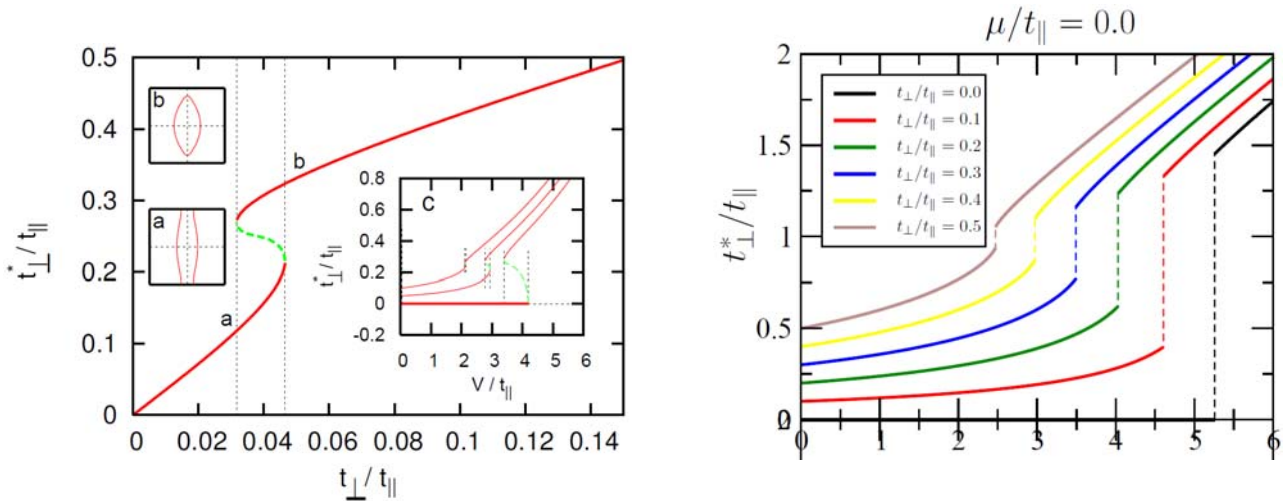


Fig. 17. Meta-nematic transition. Self-consistent Hartree Fock yields a topological Lifshitz transition from open to closed Fermi surface of first order. The conventional Lifshitz is the quantum critical endpoint of this meta-nematic transition.

Cooperations

The work on the project has been carried out in cooperation/coordination with experimental activity in CFN/KIT on carbon nanotubes --- Krupke, von Löhneysen (subproject C4.1); Kappes (C3.2) and metallic nanostructures --- von Löhneysen (B1.4, B2.7), as well with theoretical activity in the area of computational approaches (DMRG, DFT) to nonequilibrium systems --- Wölfle, Schmitteckert, Evers (B2.10) and with theoretical studies of 0D, 1D, and 2D nanostructures in subprojects B1.7 (Schön), B2.2 (Schön/Schnirman), and B2.9 (Wölfle). Further, we have been working in close contacts and cooperation with a number of leading experimental and theoretical groups worldwide: Weizmann Institute, Bar Ilan University (Israel); Exeter University, Birmingham University, Oxford University, Nottingham University, Kent University,

Loughborough University (UK); University of Gainesville, University of Chicago, University of California in Santa Barbara, Argonne National Laboratory (USA); International Centre for Theoretical Physics (Trieste, Italy); Ioffe Institute, Petersburg Nuclear Physics Institute (St. Petersburg, Russia).

References

- own work of the report period with complete titles -

- [1] T. Giamarchi, *Quantum Physics in One Dimension*, Oxford Science Publications (Oxford, 2004).
- [2] M. Bockrath, D.H. Cobden, J. Lu, A.G. Rinzler, R.E. Smalley, L. Balents, and P.L. McEuen, *Nature* **397**, 598 (1999).
- [3] J. Nygrard, D.H. Cobden, and P.E. Lindelof, *Nature* **408**, 342 (2000);
J. Wei, M. Shimogawa, Z. Wang, I. Radu, R. Dormaier, and D.H. Cobden, *Phys. Rev. Lett.* **95**, 256601 (2005);
P.J. Leek, M.R. Buitelaar, V.I. Talyanskii, C.G. Smith, D. Anderson, G.A.C. Jones, J. Wei, and D.H. Cobden, *Phys. Rev. Lett.* **95**, 256802 (2005).
- [4] Z. Yao, H. Postma, L. Balents, and C. Dekker, *Nature* **402**, 273 (1999);
H.W.Ch. Postma, T. Teepen, Z. Yao, M. Grifoni, and C. Dekker, *Science* **293**, 76 (2001)
- [5] A.F. Morpurgo, J.Kong, C.M. Marcus, and H. Dai, *Science* **286**, 263 (1999).
- [6] N. Mason, M.J. Biercuk, and C.M. Marcus, *Science*, **303**, 655 (2004).
- [7] A.Y. Kasumov, R. Deblock, M. Kociak, B. Reulet, H. Bouchiat, I.I. Khodos, Yu.B. Gorbatov, V.T. Volkov, C. Journet, and M. Burghard, *Science* **284**, 1508 (1999).
- [8] P. Jarillo-Herrero, J.A. van Dam, and L.P. Kouwenhoven, *Nature* **439**, 953 (2006).
- [9] R. Krupke, F. Hennrich, H.B. Weber, D. Beckmann, O. Hampe, S. Malik, M.M. Kappes, and H. v. Loehneysen, *Appl. Phys. A* **76**, 397 (2003).
- [10] H.R. Shea, R. Martel, and Ph. Avouris, *Phys. Rev. Lett.* **84**, 4441 (2000).
- [11] H.T. Man and A.F. Morpurgo, *Phys. Rev. Lett.* **95**, 026801 (2005).
- [12] S. Li, Z. Yu, C. Rutherglen, and P.J. Burke, *Nano Lett.* **4**, 2003 (2004).
- [13] M.S. Purewal, B.H.Hong, A.Ravi, B.Chandra, J.Hone, and P. Kim, *Phys. Rev. Lett.* **98**, 186808 (2007).
- [14] O.M. Auslaender, A. Yacoby, R. de Picciotto, K.W. Baldwin, L.N. Pfeiffer, and K.W. West, *Science* **295**, 825 (2002).
- [15] E. Levy, A. Tsukernik, M. Karpovski, A. Palevski, B. Dvir, E. Pelucchi, A. Rudra, E. Kapon, and Y. Oreg, *Phys. Rev. Lett.* **97**, 196802 (2006).
- [16] E. Slot et al., M.A. Holst, H.S.J. van der Zant, and S.V. Zaitsev-Zotov, *Phys. Rev. Lett.* **93**, 176602 (2004).
- [17] L. Venkataraman, Y.S. Hong, and P. Kim, *Phys. Rev. Lett.* **96**, 076601 (2006).
- [18] A.N. Aleshin, H.J. Lee, Y.W. Park, and K. Akagi, *Phys. Rev. Lett.* **93**, 196601 (2004).
- [19] A.N. Aleshin, *Adv. Mat.* **18**, 17 (2006).
- [20] K.S. Novoselov, A.K. Geim, S.V. Morozov, D. Jiang, M.I. Katsnelson, I.V. Grigorieva, S.V. Dubonos, and A.A. Firsov, *Nature (London)* **438**, 197 (2005).
- [21] Y. Zhang, Y.W. Tan, H.L. Stormer, and P. Kim, *Nature (London)* **438**, 201 (2005).
- [22] A.K. Geim and K.S. Novoselov, *Nature Materials* **6**, 183 (2007).
- [23] A.H. Castro Neto, F. Guinea, N.M.R. Peres, K.S. Novoselov, and A.K. Geim, arXiv:0709.1163, to appear in *Rev. Mod. Phys.*
- [24] Y.W. Tan, Y. Zhang, H.L. Stormer, and P. Kim, *Eur. Phys. J. Special Topics*, **148**, 15 (2007).

- [25] P. Debray, V. N. Zverev, V.L. Gurevich, R. Klesse and R. S. Newrock, *Semicond. Sci. Technol.* **17**, R21 (2002).
- [26] M. Pustilnik, E.G. Mishchenko, L.I. Glazman, and A.V. Andreev, *Phys. Rev. Lett.* **91**, 126805 (2003).
- [27] R. G. Pereira, J. Sirker, J.-S. Caux, R. Hagemans, J. M. Maillet, S. R. White, and I. Affleck, *Phys. Rev. Lett.* **96**, 257202 (2006) ;
S. Teber, *Eur. Phys. J. B* **52**, 233 (2006).
- [28] Y.Hosokoshi, Y. Nakazava, K.Inoue, K.Takizawa, H.Nakano, M.Takahashi, and T.Goto, *Phys. Rev. B* **60**, 12924 (1999).
- [29] B. L. Altshuler and A. G. Aronov, in “Electron-Electron Interaction In Disordered Systems”, ed. by A.L. Efros and M. Pollak (Elsevier, 1985), p.1;
A.M. Finkel'stein, *Sov. Sci. Rev. A* **14**, 1 (1990);
L.S. Levitov and A.V. Shytov, *JETP Lett.* **66**, 214 (1997).
- [30] B. Muzykantskii, N. d'Ambrumenil, and B. Braunecker, *Phys. Rev. Lett.* **91**, 266602 (2003);
D.A. Abanin and L.S. Levitov, *Phys. Rev. Lett.* **94**, 186803 (2005).
- [31] A. Rosch, J. Paaske, J. Kroha, and P. Wölfle, *Phys. Rev. Lett.* **90**, 076804 (2003);
J. Paaske, A. Rosch, P. Wölfle, N. Mason, C.M. Marcus, and J. Nygard, *Nature Physics* **2**, 460 (2006).
- [32] A. Anthore, F. Pierre, H. Pothier, and D. Esteve, *Phys. Rev. Lett.* **90**, 076806 (2003).
- [33] Y.-F. Chen, T. Dirks, G. Al-Zoubi, N. Birge, and N. Mason, *Phys. Rev. Lett.* **102**, 036804 (2009).
- [34] C. Altimiras, H. le Sueur, U. Gennser, A. Cavanna, D. Mailly, F. Pierre, *Nature Physics* **6**, 34 (2010).
- [35] D.C. Mattis and E.H. Lieb, *J. Math. Phys.* **6**, 375 (1965); M. Khodas, M. Pustilnik, A. Kamenev, and L.I. Glazman, *Phys. Rev. B* **76**, 155402 (2007).
- [36] D.B. Gutman, Y. Gefen, and A. D. Mirlin, *Non-equilibrium 1D many-body problems and asymptotic properties of Toeplitz determinants*, arXiv:1010.5645, submitted to *J. Phys. A*.
- [37] H.R. Shea, R. Martel, and Ph. Avouris, *Phys. Rev. Lett.* **84**, 4441 (2000); S. Zou et al., *Nano Lett.* **7**, 276 (2007).
- [38] V. Piazza et al., *Phys. Rev. B* **62**, 10630(R) (2000); A. Fuhrer et al., *Nature* **413**, 822 (2001); U.F. Keyser et al., *Phys. Rev. Lett.* **90**, 196691 (2003); E.B. Olshanetsky et al., *JETP Lett.* **81**, 625 (2005).
- [39] D.N. Aristov. *Constraints on conductances for Y junctions of quantum wires*, arXiv.org: 1008.1645, submitted to *Phys. Rev. B*.
- [40] S.T. Carr, B. N. Narozhny, and A.A. Nersesyan. *The effect of a local perturbation in a fermionic ladder*, arXiv.org: 1008.5282, submitted to *Phys. Rev. Lett.*